Electronic Supplementary Material (ESI) for ChemComm. This journal is © The Royal Society of Chemistry 2021

Dye-Polyoxometalate Coordination Polymer as Photodriven Electron Pump for Photocatalytic Radical Coupling Reactions

Zheng Ming,[‡a,b,c] Tiexin Zhang,[‡a*] Wenming Tian,[d] Jianing Li,[a] Zhenhui Liu,[a] Renhai Liu,[a] Zhongmin Liu,[b,c*] and Chunying Duan[a,b*]

[a]*State Key Laboratory of Fine Chemicals, Dalian University of Technology, Dalian 116024, People's P. R. China.*

E-mail: zhangtiexin@dlut.edu.cn; cyduan@dlut.edu.cn

[b]*Zhang Dayu College of Chemistry, Dalian University of Technology, Dalian 116024, P. R. China.*

E-mail: liuzm@dicp.ac.cn

[c]*National Engineering Laboratory for Methanol to Olefins, Dalian National Laboratory for Clean Energy, Dalian Institute of Chemical Physics, Chinese Academy of Sciences, Dalian, 116023, P. R. China.*

[d]*State Key Laboratory of Molecular Reaction Dynamics and Dynamics Research Center for Energy and Environmental Materials, Dalian Institute of Chemical Physics, Chinese Academy of Sciences, Dalian 116023, P. R. China.*

‡ These author contributed equally to this work.

Table of Contents

1. Experimental Section

Materials and Methods

The ligand tris[4(pyridin-4-yl)phenyl]amine (**TPPA**) was prepared according to literature procedure.[1] [(*n*-$C_4H_9)_4N]_4[\gamma$-$H_2SiV_2W_{10}O_{40}]\cdot H_2O$, the salt of Keggin POM, was synthesized according to references.[2,3] Other chemical materials were purchased from commercial sources and used without further purification unless specified.

^{1}H NMR spectra were recorded on a Varian INOVA-400 MHz type spectrometer, with TMS as internal standard.

The powder X-ray diffraction (PXRD) patterns were collected by Rigaku D/Max-2400 X-ray diffractometer with Cu *K*α radiation (λ = 1.54056 Å). Thermogravimetric analyses (TGA) were carried out at a ramp rate of 10 ^oC min^{-1} in nitrogen flow with a SDT Q600 instrument. Scanning electron micrographs (SEM) was shot by Hitachi SU8020, and energy dispersive spectrometer (EDS) analysis of the catalyst surface was conducted with Horiba X-max. Fourier transform infrared (IR) spectra were recorded using ATR mode on a Nicolet iS50 spectrometer. Liquid UV-Vis spectra were performed on a TU-1900 spectrophotometer. The solid UV−vis spectra were recorded on a Hitachi U-4100 UV−vis−NIR spectrophotometer. The fluorescent spectra were measured on JASCO FP-6500. Photoluminescence decay curves were recorded on Edinburgh FLS 920 stable/transient fluorescence spectrometer.

X-ray photoelectron spectroscopy (XPS) analysis was conducted with ThermoFisher ESCALAB250xi using monochromatized Al Kα as the exciting radiation. Binding energy of C 1s at 284.8 eV was used as a reference. In case of sampling from half-reactions as shown in Fig. S21, ESI†, the dispersed particles of specified half-reaction were collected via filtration, then transferred into the testing panel prior to XPS examinations. The sampling operations were carried out under N_2 atmosphere. Electron paramagnetic resonance (EPR) spectra were collected on Bruker E500; scanning frequency: 9.4117 GHz; test temperature: 293 K. In a typical procedure, 2 mg solid sample and 0.2 mL degassed *n*-Hexane were added into a 4 mm thin wall quartz EPR sample tube and sealed under N_2 atmosphere. The mixtures might be subjected to light radiation from a 500W Xe lamp with or without the prior addition of specified substrates. In case of sampling from half-reactions as shown in Fig. S21, ESI†, the dispersed particles of specified half-reaction were collected via filtration, transferred into EPR tube, and then re-dispersed in *n*-Hexane prior to EPR examinations. All solvents were fully degassed before use, all the operations were performed under N_2 atmosphere. The EPR simulation was conducted with Matlab easyspin (2012) software, g =1.981, $g_\perp$=1.97; A =151, $A_\perp$=63.

The femtosecond transient absorption (fs-TA) setup used for this study was based on a regenerative amplified Ti: sapphire laser system from Coherent (800 nm, 35 fs, 6 mJ $pulse^{-1}$, and 1 kHz repetition rate), nonlinear frequency mixing techniques and the Femto-TA100 spectrometer (Time-Tech Spectra). Briefly, the 800 nm output pulse from the regenerative amplifier was split in two parts with a 50% beam splitter. The transmitted part was used to pump a TOPAS Optical Parametric Amplifier (OPA) which generates a wavelength-tunable laser pulse from 250 nm to 2.5 μm as pump beam. The reflected 800 nm beam was split again into two parts. One part with less than 10% was attenuated with a neutral density filter and focused into a 2 mm thick sapphire window to generate a white light continuum (WLC) from 420 nm to 800 nm used for probe beam. The probe beam was focused with an Al parabolic reflector onto the sample (Preparation of the sample: **TPPA**-Cd-$SiW_{10}V_2$ was finely grinded and dispersed in DCM, the suspension was transferred into a quartz cuvette and its UV-visible absorbance was adjusted to 0.5 before further characterization). After the sample, the probe beam was collimated and then focused into a fiber-coupled spectrometer with CMOS sensors and detected at a frequency of 1 kHz. The delay between the pump and probe pulses was controlled by a motorized delay stage. The pump pulses were chopped by a synchronized chopper at 500 Hz and the absorbance change was calculated with two adjacent probe pulses (pump-blocked and pump-unblocked). All experiments were performed at room temperature.

Cyclic voltammogram (CV) and electrochemical impedance spectroscopy (EIS) were measured on ZAHNER ENNIUM Electrochemical Workstation with a typical three electrode system. A glassy carbon working electrode (3mm diameter), a platinum-wire counter electrode and an Ag/AgCl reference electrode were used in an aqueous acetonitrile solution of 0.1 mol L^{-1} tetrabutylammonium hexafluorophosphate (electrolyte, pH=7.5). In the case of EIS examinations, crystals of **TPPA**-Cd-$SiW_{10}V_2$ were mixed with nafion and spread onto a piece of ITO conductive glass to serve as the working electrode.

Syntheses of Coordination Polymer

Synthesis of **TPPA**-Cd-$SiW_{10}V_2$: A mixture of **TPPA** (0.05 mmol), $[(n\text{-}C_4H_9)_4N]_4[\gamma\text{-}H_2SiV_2W_{10}O_{40}].H_2O$ (0.03 mmol), $Cd(OAc)_2\bullet 2H_2O$ (0.2 mmol) were dissolved in 3 mL DMF. The resulting mixture was heated in a 25 mL Teflon-lined autoclave at 110 ^oC for 36 hrs. After cooling the autoclave to room temperature, yellow dodecahedron shaped single crystals were obtained in a yield of 50% (based on ligand **TPPA**). The crystals were washed with DMF, and dried under vacuum heating before the use as photocatalyst.

Single Crystal X-ray Crystallography of Coordination Polymer

Single-crystal X-ray intensity data were measured on a Bruker SMART APEX CCD diffractometer (Mo–Kα radiation, λ = 0.71073 Å) using the SMART[4] and SAINT[5] programs. The crystal data was solved by direct methods and further refined by full-matrix least-squares refinements on F^2 using the SHELXL *version* 2018.3 software,[6] and an absorption correction was performed using the SADABS program. SQUEEZE was used to remove the contributions of disordered solvents using PLATON software.[7] The framework formula was $C_{264}N_{32}O_{120}H_{192}Cd_6Si_3V_6W_{30}$, the amount of solvent molecular was determined by the thermogravimetric analysis (TGA) to show a solvent desorption weightlessness of 9.2%, which was correlated to 17 molecules of solvent DMF for each unit of framework.

Table S1. Crystal data and structure refinements.

Compound	**TPPA**-Cd-$SiW_{10}V_2$
Empirical formula	$C_{264}N_{32}O_{120}H_{192}Cd_6Si_3V_6W_{30}$. 17($C_3H_7NO$)
Formula weight	13554.92
T/K	220
Crystal system	Cubic
Space group	*Im-3m*
a/Å	29.8105
b/Å	29.8105
c/Å	29.8105
α/°	90
β/°	90
γ/°	90
V/Å^3	26492
Z	2
D_{calc}/g cm^{-3}	1.699
μ/mm^{-1}	6.889
F(000)	12656.0
Data completeness	0.999
R_{int}	0.0497
R_{sigma}	0.0132
GOF	1.064
R [$I > 2\sigma(I)$] [a]	R_1 = 0.0776
	wR_2 = 0.2039
R indices (all data) [b]	R_1 = 0.1035
	wR_2 = 0.2385
CCDC number	2036124

[a] $R_1 = \Sigma||F_o| - |F_c||/\Sigma|F_o|$; [b] $wR_2 = \Sigma[w(F_o^2 - F_c^2)^2]/\Sigma[w(F_o^2)^2]^{1/2}$

2. Supplementary Structural Figures

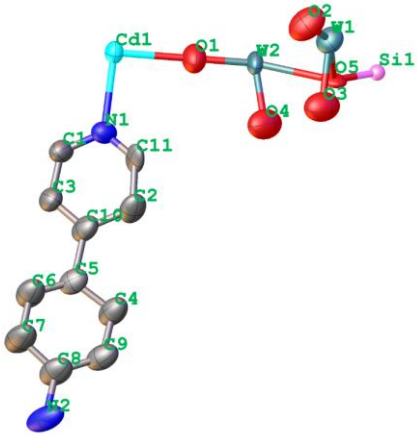

Fig. S1. Ellipsoid diagram of **TPPA**-Cd-$SiW_{10}V_2$ in an asymmetric unit with labelling scheme (50% probability). Selective bond distance in **TPPA**-Cd-$SiW_{10}V_2$ (Symmetry code: #1 1-Z, +Y, -1+X; #2 +X, +Y, -Z; #3 +X, 1-Y, -Z): W(1)-O(2) 1.646, W(1)-O(3)$^{\#1}$ 1.890, W(1)-O(4)$^{\#2}$ 1.889, W(2)-O(1) 1.72, W(2)-O(4)$^{\#3}$ 1.891, Si(1)-O(5) 1.60, Cd(1)-O(1) 2.27, Cd(1)-N(1) 2.30.

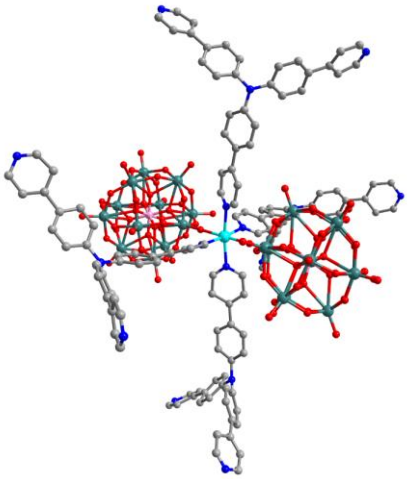

Fig. S2. Diagram of the coordination environment of Cd^{2+} within **TPPA**-Cd-$SiW_{10}V_2$.

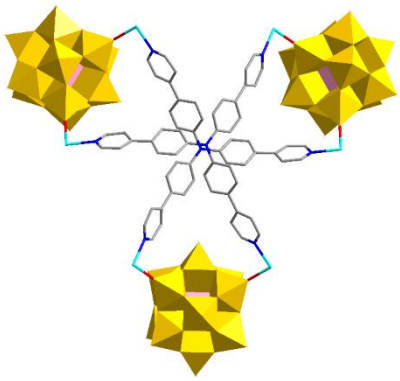

Fig. S3. Diagram of the coordination environment of **TPPA** within **TPPA**-Cd-$SiW_{10}V_2$.

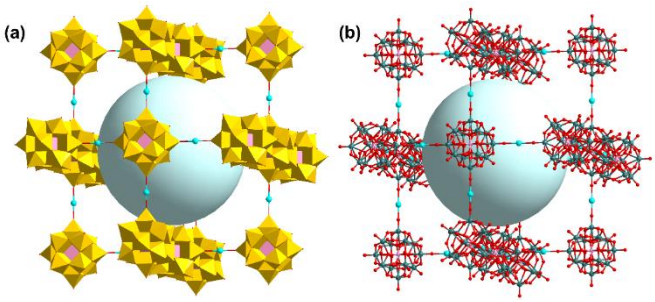

Fig. S4 Connecting mode of POM $SiW_{10}V_2$ moiety within **TPPA**-Cd-$SiW_{10}V_2$: (a) polyhedron (b) ball-and-stick representation.

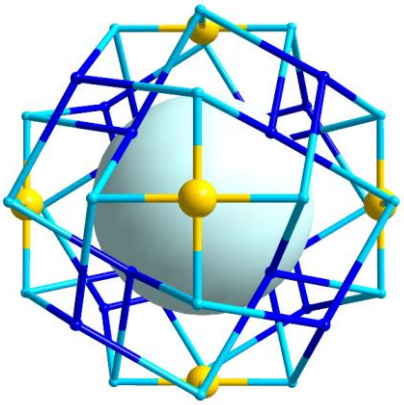

Fig. S5. A simplified view of the octahedral cage in **TPPA**-Cd-$SiW_{10}V_2$.

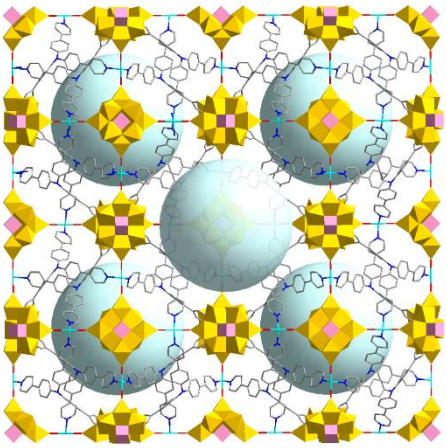

Fig. S6. View of the three-dimensional framework of **TPPA**-Cd-$SiW_{10}V_2$ showing the interconnection of octahedral cages.

3. Characterization of Coordination Polymer

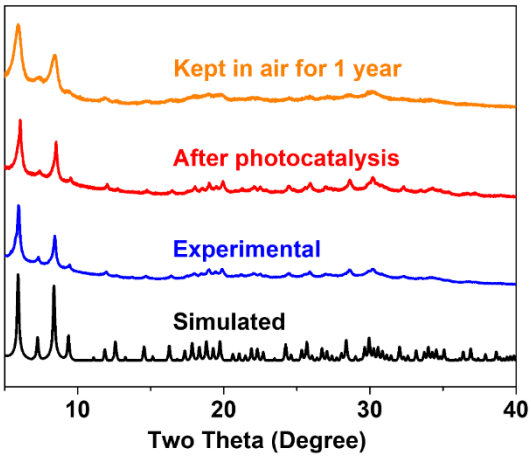

Fig. S7. PXRD patterns of **TPPA**-Cd-$SiW_{10}V_2$: simulated (black), experimental (blue), recycled catalyst after reactions (red), and kept in air for 1 year (yellow).

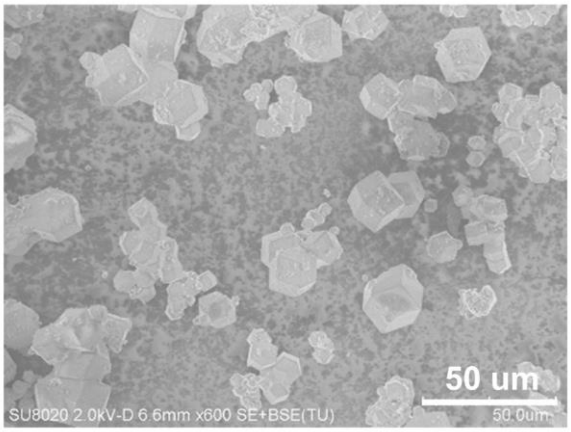

Fig. S8. SEM images show the dodecahedron shaped crystals of **TPPA**-Cd-$SiW_{10}V_2$.

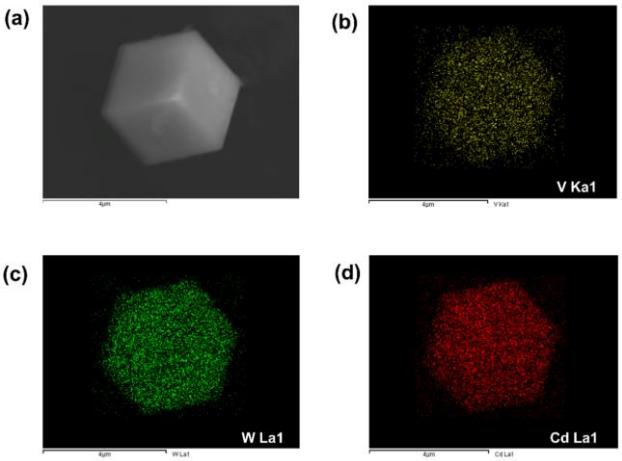

Fig. S9. Energy dispersive spectroscopy (EDS) analysis of **TPPA**-Cd-$SiW_{10}V_2$ showing the selected crystal (a) and the element distribution of V (b), W (c) and Cd (d), respectively.

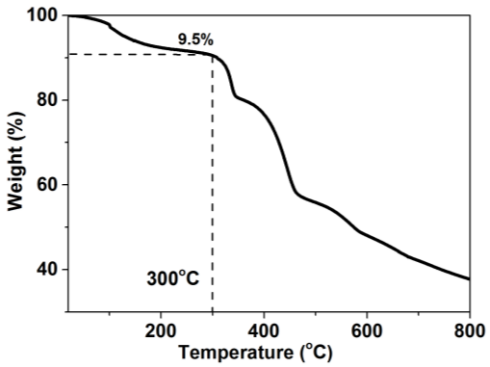

Fig. S10. Thermogravimetric analysis (TGA) curve of **TPPA**-Cd-$SiW_{10}V_2$ under N_2 atmosphere. The weight loss of 9.5%. from 25 °C to 300 °C could be attributed to the desorption of DMF molecules.

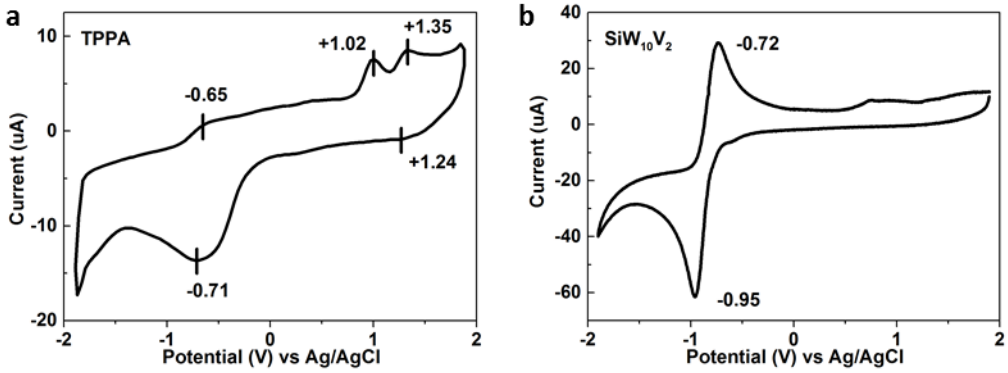

Fig. S11. (a) Cyclic voltammograms (CV) of free ligand **TPPA**, solvent:CH_3CN. The redox potential around +1.02 V could be assigned to E(**TPPA**$^{+\cdot}$/**TPPA**), and the pair of peaks at +1.24 V and +1.35 V might be ascribed to E(**TPPA**$^{2+}$/**TPPA**$^{+\cdot}$).[7] (b) Cyclic voltammograms (CV) of POM $SiW_{10}V_2$, solvent: CH_3CN.

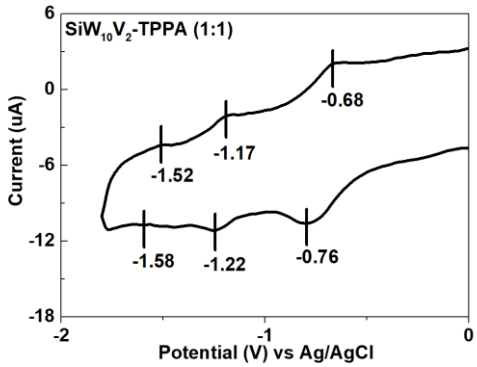

Fig. S12. Cyclic voltammograms (CV) of POM $SiW_{10}V_2$, upon the addition of 1 equiv. amount of free ligand **TPPA**, solvent: CH_3CN.

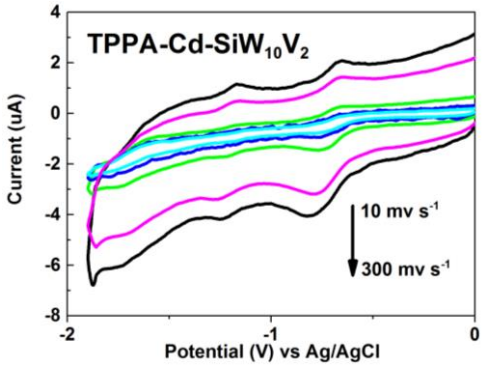

Fig. S13. Cyclic voltammograms (CV) of **TPPA**-Cd-$SiW_{10}V_2$ at scan rate of 300, 200, 50, 20, 10 mv/s (solvent: CH_3CN).

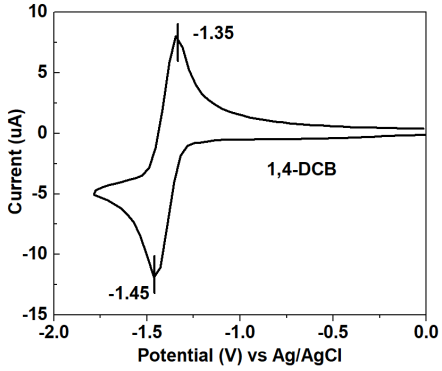

Fig. S14. CV curves of 1,4-DCB **1b** exhibiting the $E_{1/2red}$ = *ca*. -1.45 V, solvent: CH_3CN.

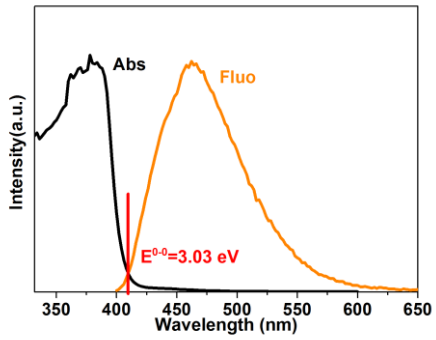

Fig. S15. Absorption (black line) and emission spectra (yellow line) of free ligand **TPPA**, excited at 380 nm.

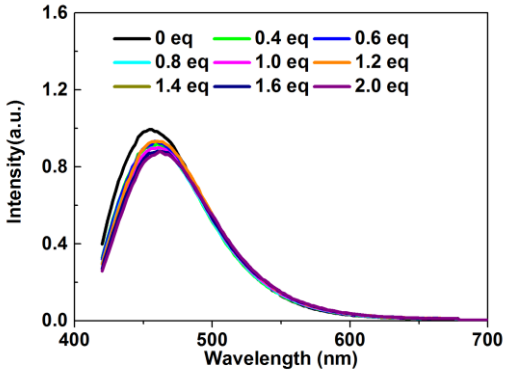

Fig. S16.-The emission quenching experiment of free ligand **TPPA** in DMA upon the addition of POM $SiW_{10}V_2$, excited at 380 nm.

4. Comparative EPR Study:

TPPA-Cd-$SiW_{10}V_2$ was treated with excess amount of electron-donating substrate **1a** and successive photoirradiation for 1h, the EPR spectrum did not show any peaks correlated to W^{5+} species, but only exhibited the signals of V^{4+}, which was in accordance with the simulated EPR data as shown in Fig. S17, ESI†. Furthermore, after adding the electron-accepting substrate 1,4-dicyanobenzene (1,4-DCB) **2a** to this mixture, the EPR peaks of V^{4+} was remarkably quenched.

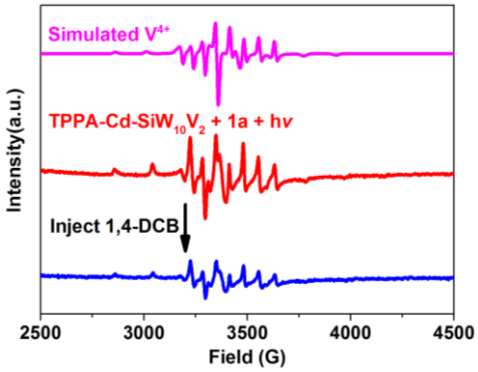

Fig. S17. Comparison between the simulated (pink), experimental Radiated **1a**@**TPPA**-Cd-$SiW_{10}V_2$ (red) spectra, and the spectrum after injecting 1,4-DCB (blue).

5. Comparative XPS Study:

The free ligand **TPPA** exhibited N1s peaks of triphenylamine (**TPA**) core and uncoordinated pyridyl terminal at 399.9 and 398.8, respectively. After the assembly of free **TPPA** ligand into coordination polymer **TPPA**-Cd-$SiW_{10}V_2$, the N1s signal of pyridyl terminal (398.8) vanished, the pyridyl coordinated with Cd ion was found at 406.2 and overlapped with the peak of $Cd3d_{5/2}$.

Owing to the spontaneous intraframework partial charge transfer from ligand **TPPA** to POM moiety and the possible background irradiation from daylight during the storage of **TPPA**-Cd-$SiW_{10}V_2$, N1s peak of the radical cationic **TPPA**$^{+\cdot}$ emerged at 401.9. Accordingly, the bands of $V2p_{1/2}$ and W4f of POM moiety shifted slightly towards the smaller values after assembling POM moieties into **TPPA**-Cd-$SiW_{10}V_2$, indicating the partial electron transfer from **TPPA** to POM unit within **TPPA**-Cd-$SiW_{10}V_2$. The long-lived charge-separated pairs at ground state implied the successful structural design for retarding the undesirable back electron transfer, which ensured the unidirectional electron transfer route from external electron-donating to electron-accepting substrates mediated by the function of "photodriven electron pump" upon irradiation.

After adding the electron-donating substrate **1a** to the coordination polymer and the successive photoirradiation, the N1s peak of radical cationic species with binding energy of 401.9 eV vanished; N1s peaks of the neutral triphenylamine (**TPA**) moiety and the pyridyl coordinated with Cd ion also shifted slightly towards smaller values, which were affected by the incoming exogeneous electrons contributed by **1a**; At the same time, the binding energy of $V2p_{1/2}$ dramatically decreased from 523.6 eV to 523.1 eV while that of W4f just decreased about 0.1~0.2 eV, which indicated the exogeneous electron mainly reduced V other than W upon irradiation.

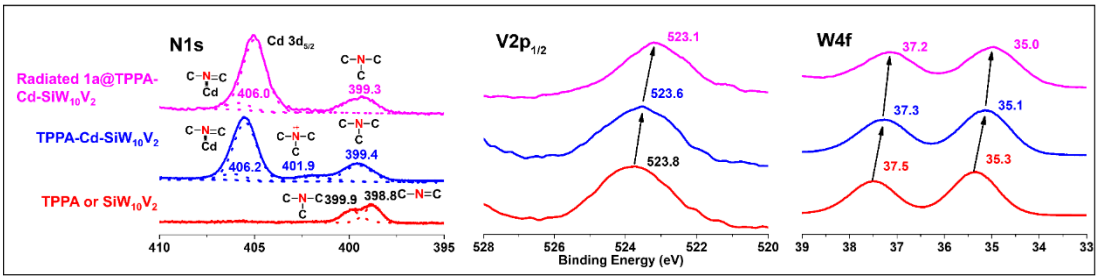

Fig. S18. Comparison of narrow-scan X-ray photoelectron spectroscopy (XPS) of **TPPA** or $SiW_{10}V_2$ (red), **TPPA**-Cd-$SiW_{10}V_2$ (blue), and **1a**@**TPPA**-Cd-$SiW_{10}V_2$.

6. Dye Uptake Experiment of TPPA-Cd-$SiW_{10}V_2$:

TPPA-Cd-$SiW_{10}V_2$ (2 mg) was soaked in a methanol solution of 2′,7′-dichorofluorescein dye (24 mM, 2 mL) overnight. The resulting crystals were washed with methanol thoroughly to remove any dye from the crystal surface until the solution become colourless, and then dried under a stream of N_2. The dried samples were digested by concentrated hydrochloric acid, and the relevant clear solution with the light of olivine colour was diluted to 25 mL and adjusted to a pH of 0.2. Absorption experiment was performed on a UV-vis TU-1900 spectrophotometer. The concentration of 2′,7′-dichlorofluorescein dye was determined by comparing the UV-vis absorption with a standard curve.

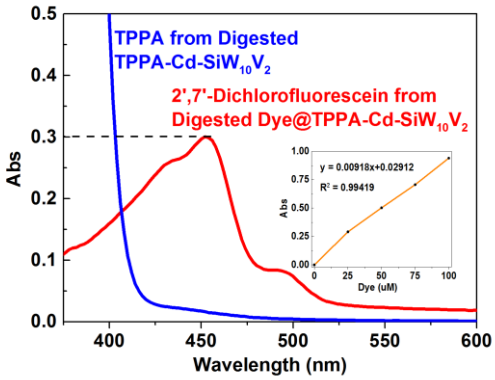

Fig. S19. UV-vis measurements of 2′,7′-dichlorofluorescein dye released from **TPPA**-Cd-$SiW_{10}V_2$; inside: The standard linear relationship between the absorption and the concentration.

7. Substrate Inclusion Experiment of TPPA-Cd-$SiW_{10}V_2$:

TPPA-Cd-$SiW_{10}V_2$ (20 mg) was soaked in DMA solution of **1a** (1.0 M, 1 mL) overnight. The resulting crystals (**1a@TPPA**-Cd-$SiW_{10}V_2$) were rinsed with DMA on a filter paper to remove residual substrate on the crystal surface, and then dried under a stream of N_2 prior to further examinations by IR or NMR. The sample was digested with one drop of DCl and dissolved in d^6-DMSO, then ^{1}H-NMR was tested.

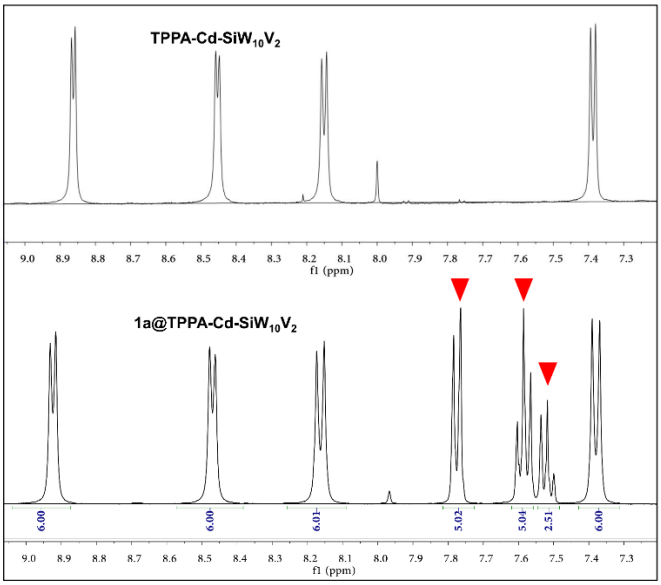

Fig.S20. ^{1}H NMR comparison of digested **TPPA**-Cd-$SiW_{10}V_2$ and **1a@TPPA**-Cd-$SiW_{10}V_2$. The comparison revealed that **TPPA**-Cd-$SiW_{10}V_2$ could adsorb approximately 2.5 equiv. of **1a** per unit (as depicted by ratio of 2.5:1.0 for **1a**/**TPPA** ligand). Peaks of **1a** were marked by reversed red triangles.

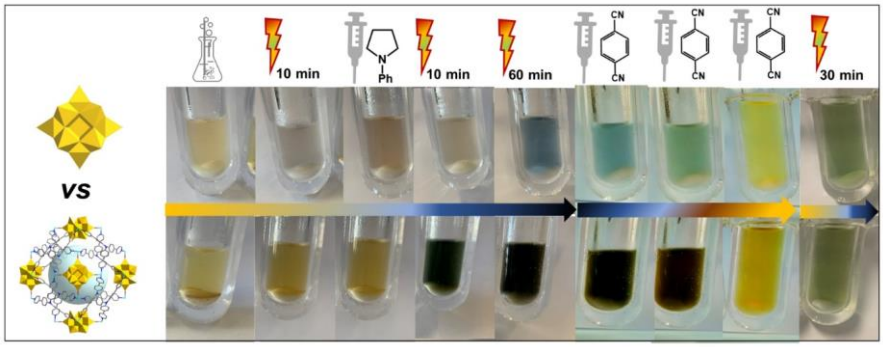

Fig. S21. Colour changes of photocatalytic successive half-reactions with the intermittent feeding of substrates **1a** and **2a** by using **TPPA**-Cd-$SiW_{10}V_2$ or homogeneous counterparts as photocatalyst.

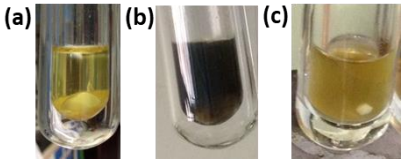

Fig. S22. Colour changes of photocatalytic one pot whole reaction by using **TPPA**-Cd-$SiW_{10}V_2$. (a) Yellow suspension of **TPPA**-Cd-$SiW_{10}V_2$, amine substrate **1a**, aryl nitrile **2a**, and NaOAc in DMA. (b) The suspension changed to deep blue after irradiation of Xe lamp. (c) The colour changed back to yellow after exposing the suspension to the air.

8. Perspective of Photocatalytic Mechanism

A mechanistic perspective of reaction was proposed according to literatures and shown in Fig. S23, ESI†. Upon photoirradiation, **TPPA** moiety of **TPPA**-Cd-$SiW_{10}V_2$ was excited to **TPPA*** ($E_{1/2ox}$ = *ca*. -2.01 V vs Ag/AgCl), which reduced $SiW_{10}V_2$, the adjacent electron relay. The concomitantly generated radical cationic **TPPA**$^{+\cdot}$ ($E_{1/2red}$ = +1.48 V *vs* Ag/AgCl, Fig. 1b) status of ligand could abstract an electron[8] upon encountering with electron-donating substrate *N*-Phenylpyrolidine **1a**, to afford amine radical cationic form of **1a** and regenerate the neutral **TPPA** motif. The neutral ligand was then excited and deeply reduced $SiW_{10}V_2$ into heteropolyblue by several rounds of PET process. The *in situ* generated heteropolyblue was a powerful reductant, which donated electrons to the encountered electron-accepting substrate 1,4-DCB **2a** ($E_{1/2red}$ = -1.45 V, Fig. S14, ESI†) (or alternatively transferred electron to O_2 under aerobic atmosphere) to form the corresponding radical anion of **1b** as well as retrieving POM, thus furnishing a cycle of unidirectional photodriven electron pumping process. The amine radical cation would be transformed to *α*-amino radical upon deprotonation by base,[9] then, a radical-radical coupling could occur to generate the *α*-aryl amine **3a** after a spontaneous releasement of cyanide (or give the formation of *α*-carbonylation product **4a** under aerobic condition without using **2a**).

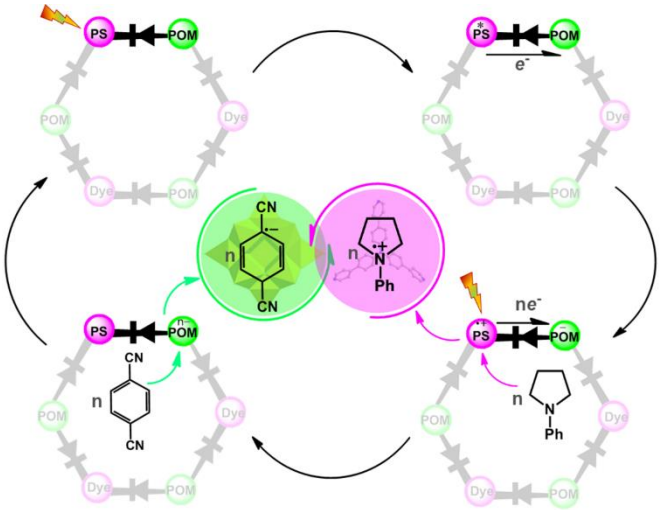

Fig. S23. Proposed reaction route of photoinduced electron pump for radical coupling.

9. Typical Procedure for Photocatalysis by TPPA-Cd-$SiW_{10}V_2$

Aryl nitrile **2** (0.5 mmol, 1.0 equiv.), amine **1** (1.5 mmol, 3.0 equiv.), **TPPA**-Cd-$SiW_{10}V_2$ (3.0×10^{-4} mmol, 6.0×10^{-4} equiv.), and NaOAc (1.0 mmol, 2.0 equiv.) were added to a predried Pyrex tube equipped with a cooling water system, a rubber septum, and a stirrer, then this mixture was subjected to three cycles of vacuum and nitrogen purge. After adding degassed anhydrous DMA (2 mL), the reaction mixture was stirred and irradiated by Xe light source (500 W) under N_2 atmosphere at room temperature for 24 hrs. After the reaction, the catalyst was recovered by centrifugation and filtration, and the filtrate was concentrated under reduced pressure. The radical coupling product was isolated *via* flash chromatography on silica gel from the crude mixture.

In the case of using O_2 instead of aryl nitrile **2**, the photocatalysis was performed similarly but under an aerobic atmosphere.

Table S2. Control experiments.

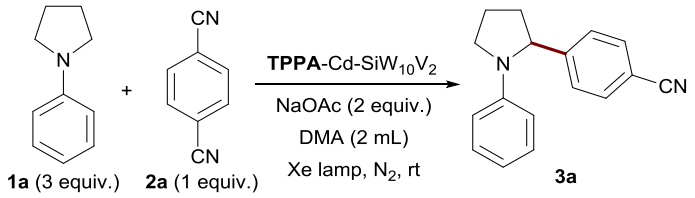

Entry[a]	Variants	Isolated Yield (%)
1	None	92
2	No Catalyst	ND
3[b]	**TPPA** as catalyst	trace
4[b]	$[(C_4H_9)_4N]_4[\gamma\text{-}H_2SiW_{10}V_2O_{40}]$ as catalyst	trace
5[b]	$Cd(OAc)_2\bullet2H_2O$ as catalyst	ND
6[b]	**TPPA** + $[(C_4H_9)_4N]_4[\gamma\text{-}H_2SiW_{10}V_2O_{40}]$	trace
7	Under Dark	ND

[a] Under general protocols described above. [b] The loading amounts of catalysts were the same as those of corresponding fragments within **TPPA**-Cd-$SiW_{10}V_2$. ND = not determined.

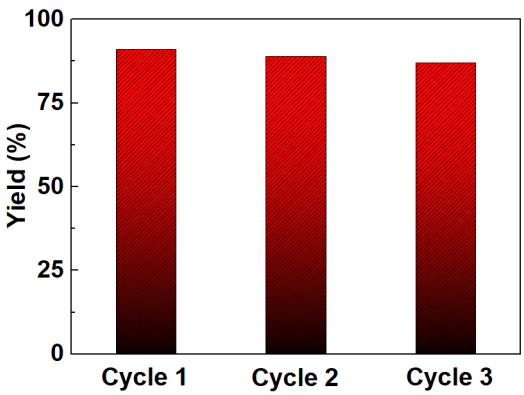

Fig. S24. Column Chart of reuse experiments of **TPPA**-Cd-$SiW_{10}V_2$ in photocatalsis.

Table S3. Detailed information of Photocatalytic radical coupling reactions.[a]

Entry	Amine **1**	Aryl Nitrile **2**	Targeted Product **3**	Isolated Yield (%)
1	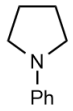 **1a**	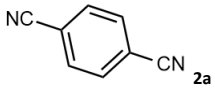 **2a**	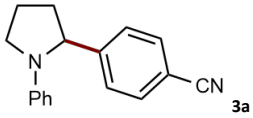 **3a**	92
2	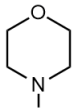 **1b**	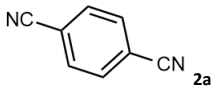 **2a**	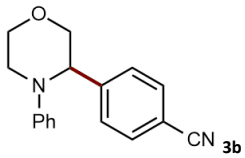 **3b**	82
3	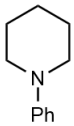 **1c**	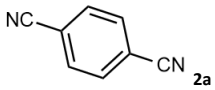 **2a**	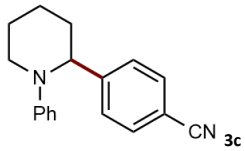 **3c**	90
4	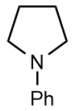 **1a**	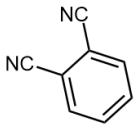 **2b**	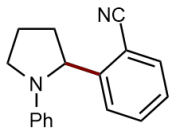 **3d**	86
5	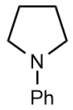 **1a**	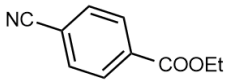 **2c**	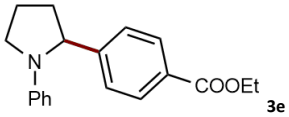 **3e**	78
6	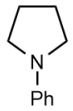 **1a**	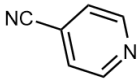 **2d**	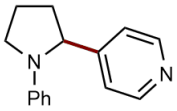 **3f**	85
7	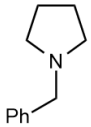 **1d**	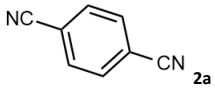 **2a**	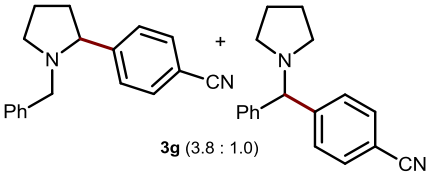 **3g** (3.8 : 1.0)	46

[a] Reaction conditions: Aryl nitriles **2** (0.5 mmol, 1.0 equiv.), amines **1** (1.5 mmol, 3.0 equiv.), **TPPA**-Cd-$SiW_{10}V_2$ (3.0×10^{-4} mmol, 6.0×10^{-4} equiv.), NaOAc (1.0 mmol, 2.0 equiv.), DMA (2 mL), 500 W Xe lamp, room temperature (rt), N_2 atmosphere, 24 h. Isolated yields.

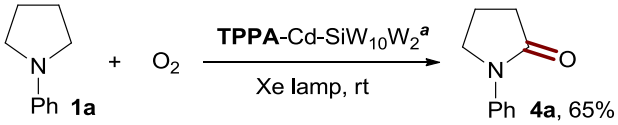

Scheme S1. Carbonation of **1a**. Reaction conditions: amine **1a** (1.5 mmol, 3.0 equiv.), **TPPA**-Cd-$SiW_{10}V_2$ (3.0×10^{-4} mmol, 6.0×10^{-4} equiv.), NaOAc (1.0 mmol, 2.0 equiv.), DMA (2 mL), 500 W Xe lamp, room temperature (rt), O_2 atmosphere, 24 h. Isolated yields.

10. NMR Data of the Products.

4-(1-Phenylpyrrolidin-2-yl)benzonitrile (3a)

^{1}H NMR (400 MHz, $CDCl_3$) δ 7.58 – 7.56 (d, J = 8.4 Hz, 2H, Ar<u>H</u>), 7.34-7.32 (d, J = 8.0 Hz, 2H, Ar<u>H</u>), 7.16-7.12 (dd, J = 8.8, 7.2 Hz, 2H, Ar<u>H</u>), 6.70-6.65 (m, 1H, Ar<u>H</u>), 6.44-6.42 (m, 2H, Ar<u>H</u>), 4.73 (dd, J = 8.4, 2.0 Hz, 1H, C<u>H</u>(Ph-4-CN)), 3.75-3.70 (m, 1H, C<u>H</u>$_A$H$_B$N), 3.45-3.39 (m, 1H, CH$_A$<u>H</u>$_B$N), 2.48-2.38 (m, 1H, C<u>H</u>$_A$CH$_B$CH(Ph-4-CN)), 2.05-1.87 (m, 3H, CH$_A$C<u>H</u>$_B$CH(Ph-4-CN)). **^{13}C NMR** (126 MHz, $CDCl_3$) δ 150.62 (C_{Ar}), 146.83 (C_{Ar}), 132.55 (C_{Ar}), 129.24 (C_{Ar}), 126.88 (C_{Ar}), 119.05 (C_{Ar}), 116.62 (C_{Ar}), 112.57 (C_{Ar}), 110.71 (CN), 62.89 (<u>C</u>H(Ph-4-CN)), 49.35 (N<u>C</u>H$_2$), 35.99 (NCH$_2$CH$_2$<u>C</u>H$_2$), 23.25 (NCH$_2$<u>C</u>H$_2$).

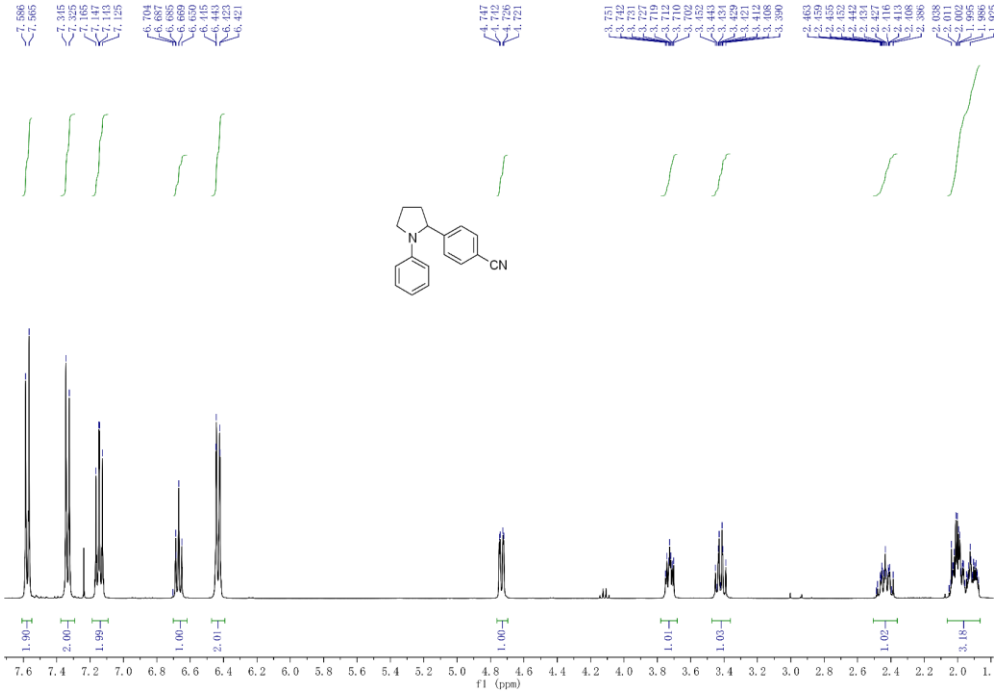

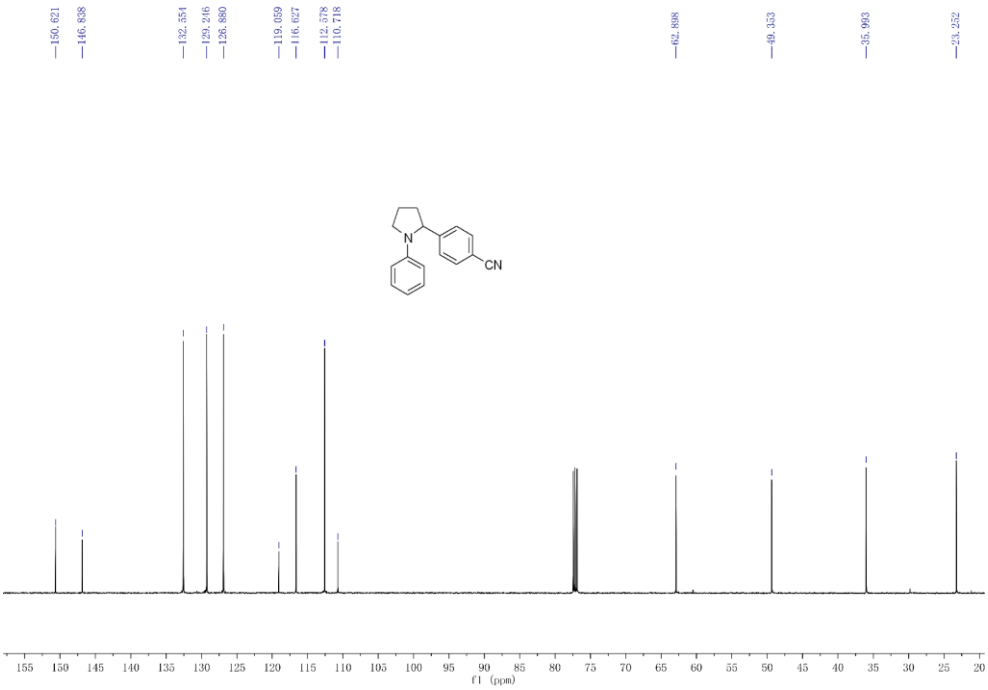

4-(4-Phenylmorpholin-3-yl)benzonitrile (3b)

^{1}H NMR (400 MHz, CDCl3) δ 7.49-7.47 (d, *J* = 8.8 Hz, 2H**,** Ar<u>H</u>), 7.43-7.40 (d, *J* = 8.4 Hz, 2H**,** Ar<u>H</u>), 7.17-7.13 (m, 2H**,** Ar<u>H</u>), 6.89-6.86 (m, 3H**,** Ar<u>H</u>), 4.43-4.40 (dd, *J* = 8.0, 3.6 Hz, 1H, C<u>H</u>(Ph-4CN)), 3.99-3.94 (m, 3H, C<u>H</u>$_A$CH$_B$CH(Ph-4-CN) and C<u>H</u>$_2$CH$_2$N), 3.64-3.59 (dd, *J* = 11.6, 8.0 Hz,1H, CH$_A$C<u>H</u>$_B$CH(Ph-4-CN)), 3.43-3.38 (m, 1H, C<u>H</u>$_A$H$_B$N), 3.15-3.08 (m, 1H, CH$_A$<u>H</u>$_B$N). **^{13}C NMR** (12**6** MHz, CDCl$_3$) *δ* 152.06 (C$_{Ar}$), 146.76 (C$_{Ar}$), 133.93 (C$_{Ar}$), 130.17 (C$_{Ar}$), 128.69 (C$_{Ar}$), 122.45 (C$_{Ar}$), 121.18 (C$_{Ar}$), 118.78 (C$_{Ar}$), 111.16 (CN), 72.71 (<u>C</u>H$_2$CH(Ph-4-CN)), 67.65 (NCH$_2$<u>C</u>H$_2$), 61.46 (<u>C</u>H(Ph-4-CN)), 52.66 (N<u>C</u>H$_2$).

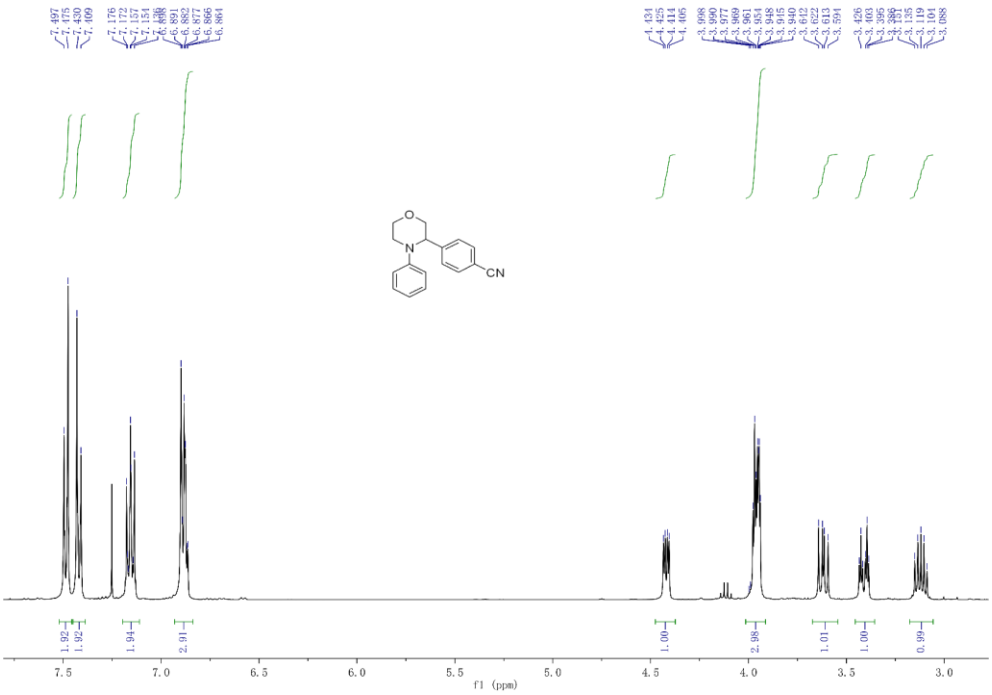

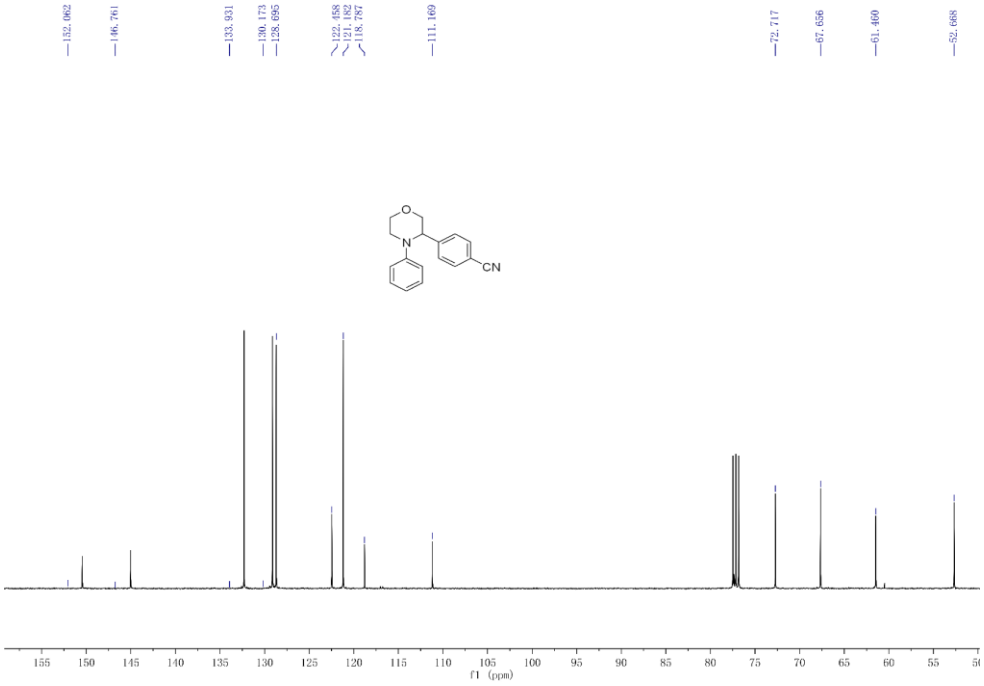

4-(1-Phenylpiperidin-2-yl)benzonitrile (3c)

^{1}H NMR (400 MHz, CDCl3) δ 7.48-7.46 (d, *J* = 8.4 Hz, 2H, Ar<u>H</u>), 7.38-7.36 (d, *J* = 8.0 Hz, 2H, Ar<u>H</u>), 7.14-7.10 (dd, *J* = 8.4, 7.2 Hz, 2H, Ar<u>H</u>), 6.87-6.85 (d, 8.0 Hz, 2H, Ar<u>H</u>), 6.82-6.78 (t, *J* = 7.6 Hz, 1H, Ar<u>H</u>), 4.40-4.37 (dd, *J* = 8.0, 3.6 Hz, 1H, C<u>H</u>(Ph-4-CN)), 3.45-3.37 (ddd, *J* = 12.0, 9.6 ,4.8 Hz, 1H, C<u>H</u>$_A$H$_B$N), 3.14-3.05 (ddd, *J* = 12.4, 7.2, 4.8 Hz 1H, CH$_A$<u>H</u>$_B$N), 2.00-1.93 (m, 1H, C<u>H</u>$_A$CH$_B$CH(Ph-4-CN)), 1.83-1.66 (m, 4H, C<u>H</u>$_2$CH$_2$N, C<u>H</u>$_A$CH$_B$CH$_2$CH$_2$N and CH$_A$C<u>H</u>$_B$CH(Ph-4-CN)), 1.58-1.48 (m, 1H, CH$_A$C<u>H</u>$_B$CH$_2$CH$_2$N). **^{13}C NMR** (126 MHz, CDCl$_3$) *δ* 151.72 (C$_{Ar}$), 150.11 (C$_{Ar}$), 132.28 (C$_{Ar}$), 129.01 (C$_{Ar}$), 128.08 (C$_{Ar}$), 121.14 (C$_{Ar}$), 120.23 (C$_{Ar}$), 120.34 (C$_{Ar}$), 119.10 (C$_{Ar}$), 110.21 (CN), 61.97 (<u>C</u>H(Ph-4-CN)), 52.76 (N<u>C</u>H$_2$), 34.44 (<u>C</u>H$_2$CH$_2$N or <u>C</u>H$_2$CH(Ph-4-CN)), 25.82 (<u>C</u>H$_2$CH$_2$N or <u>C</u>H$_2$CH(Ph-4-CN)), 22.75 (C<u>H</u>$_2$CH$_2$CH$_2$N).

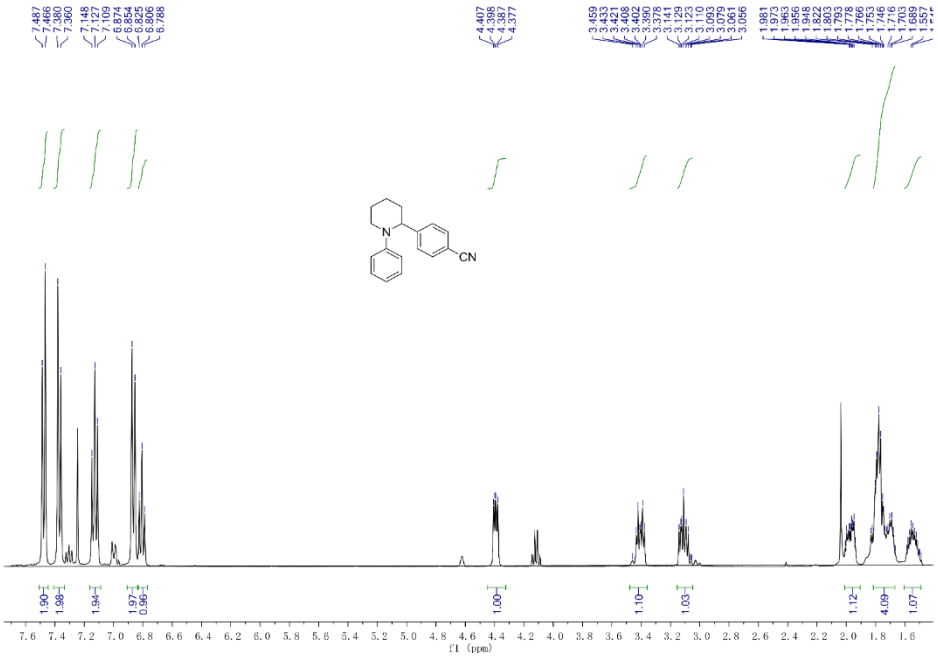

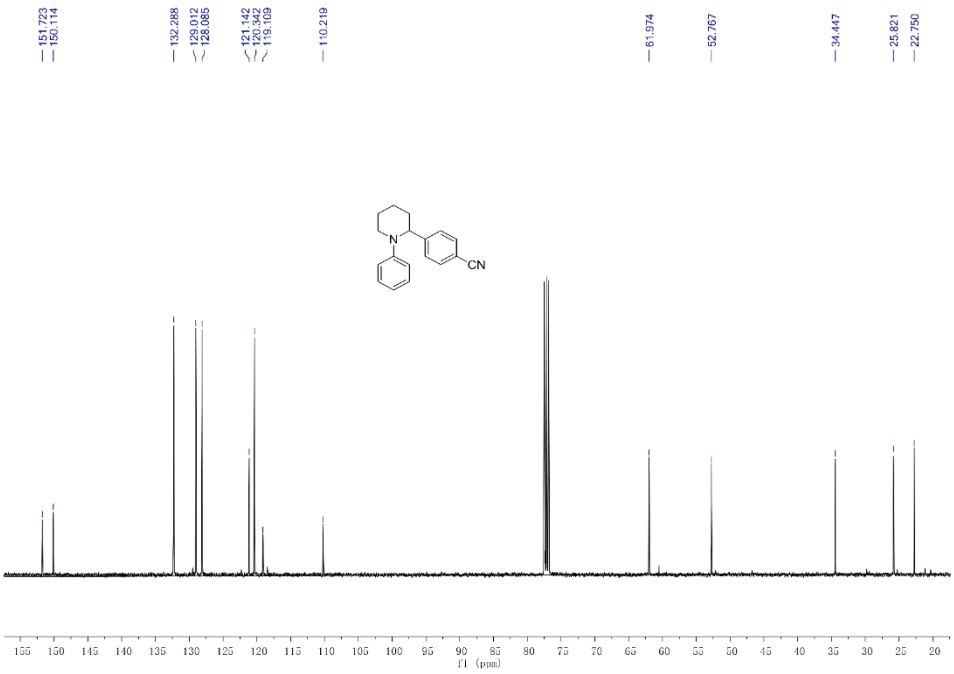

2-(1-Phenylpyrrolidin-2-yl)benzonitrile (3d)

^{1}H NMR (400 MHz, $CDCl_3$) δ 7.69 – 7.67 (d, J = 7.2 Hz, 1H, Ar<u>H</u>), 7.44-7.47 (t, J = 7.2 Hz, 1H, Ar<u>H</u>), 7.32-7.28 (m, 2H, Ar<u>H</u>), 7.16-7.13 (m, 2H, Ar<u>H</u>), 6.69-6.65 (t, J = 6.8 Hz, 1H, Ar<u>H</u>), 6.44-6.42 (d, J = 7.6 Hz, 2H, Ar<u>H</u>), 5.05-5.03 (d, J = 8.0 Hz, 1H, C<u>H</u>(Ph-2-CN)), 3.83-3.72 (m, 1H, C<u>H</u>$_A$H$_B$N), 3.46-3.44 (m, 1H, CH$_A$<u>H</u>$_B$N), 2.61-2.49(m, 1H, C<u>H</u>$_A$CH$_B$CH(Ph-2-CN)), 2.04-1.99 (m, 3H, CH$_A$C<u>H</u>$_B$CH(Ph-2-CN) and C<u>H</u>$_2$CH$_2$N). **^{13}C NMR** (126 MHz, $CDCl_3$) δ 149.14 (C_{Ar}), 146.61 (C_{Ar}), 133.72 (C_{Ar}), 133.08 (C_{Ar}), 129.24 (C_{Ar}), 127.43 (C_{Ar}), 126.95 (C_{Ar}), 117.80 (C_{Ar}), 116.72 (C_{Ar}), 112.66 (C_{Ar}), 110.22 (CN), 61.66 (<u>C</u>H(Ph-2-CN)), 49.51 (N<u>C</u>H$_2$), 35.43 (NCH$_2$CH$_2$<u>C</u>H$_2$), 23.41 (NCH$_2$<u>C</u>H$_2$).

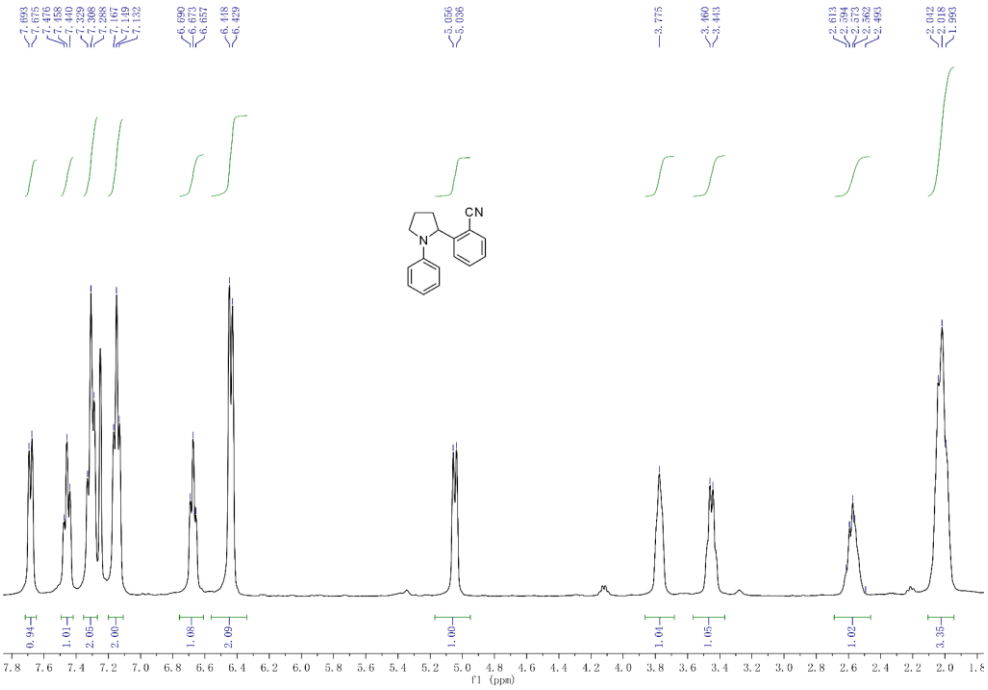

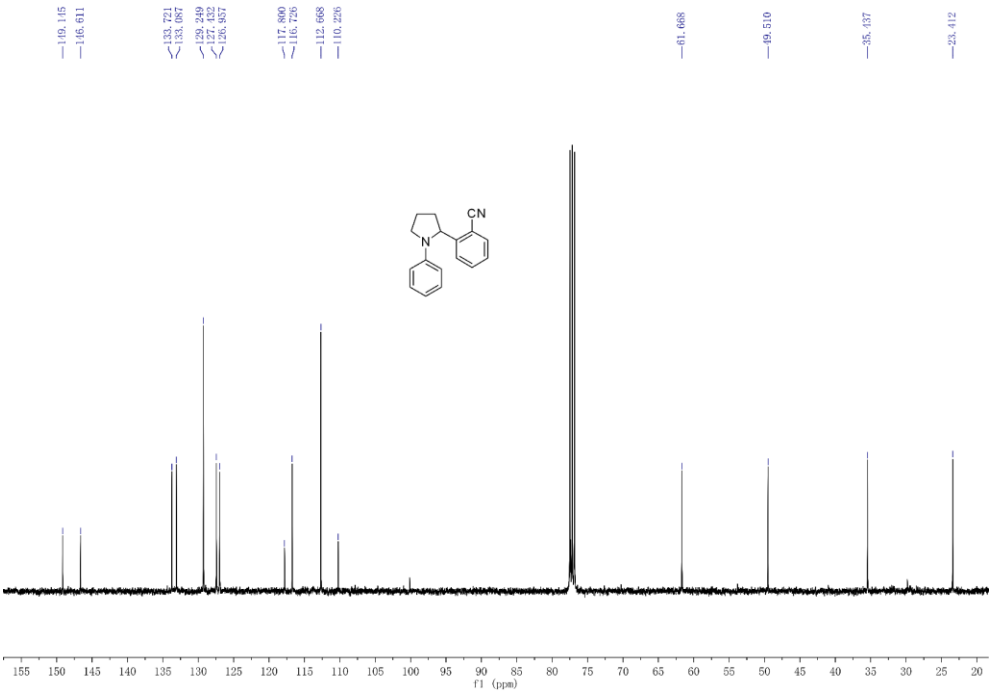

4-(1-phenylpyrrolidin-2-yl)benzoate (3e)

^{1}H NMR (400 MHz, CDCl3) δ 7.98-7.96 (d, *J* = 8.4 Hz, 2H, Ar<u>H</u>), 7.30-7.28 (d, *J* = 8.0 Hz, 2H, Ar<u>H</u>), 7.17-7.11 (dd, *J* = 8.4, 7.6 Hz, 2H, Ar<u>H</u>), 6.66-6.62 (t, *J* = 7.2Hz, 1H, Ar<u>H</u>), 6.46-6.44 (d, *J* = 8.0 Hz, 2H, Ar<u>H</u>), 4.76-4.73 (dd, *J* = 8.8, 2.0 Hz, 1H, C<u>H</u>(Ph-4-CO_2Et)), 4.38-4.32 (q, *J* = 7.2 Hz, 2H, $C\underline{H}_2CH_3$), 3.75-3.70 (m, 1H, $C\underline{H}_AH_BN$), 3.45-3.39 (m, 1H, $CH_A\underline{H}_BN$), 2.44-2.34 (1H, m , $C\underline{H}_ACH_BCH$(Ph-4-CO_2Et)), 2.02-1.97 (m, 2H,$C\underline{H}_2CH_2N$), 1.93-1.86 (1H, m , $CH_AC\underline{H}_BCH$(Ph-4-CO_2Et)), 1.35 (3H, t, *J* = 7.0 Hz, $CH_2C\underline{H}_3$). **^{13}C NMR** (126 MHz, $CDCl_3$) *δ* 166.63 (<u>C</u>O_2Et), 150.27 (C_{Ar}), 147.07 (C_{Ar}), 130.02 (C_{Ar}), 129.17 (C_{Ar}), 126.05 (C_{Ar}), 116.27 (C_{Ar}), 112.54 (CN), 63.01 ($CO_2\underline{C}H_2CH_3$), 60.94 (<u>C</u>H(Ph-4-CO_2Et)), 49.32 ($N\underline{C}H_2$), 36.09 ($NCH_2CH_2\underline{C}H_2$), 23.29 ($NCH_2\underline{C}H_2$), 14.47 ($CO_2CH_2\underline{C}H_3$).

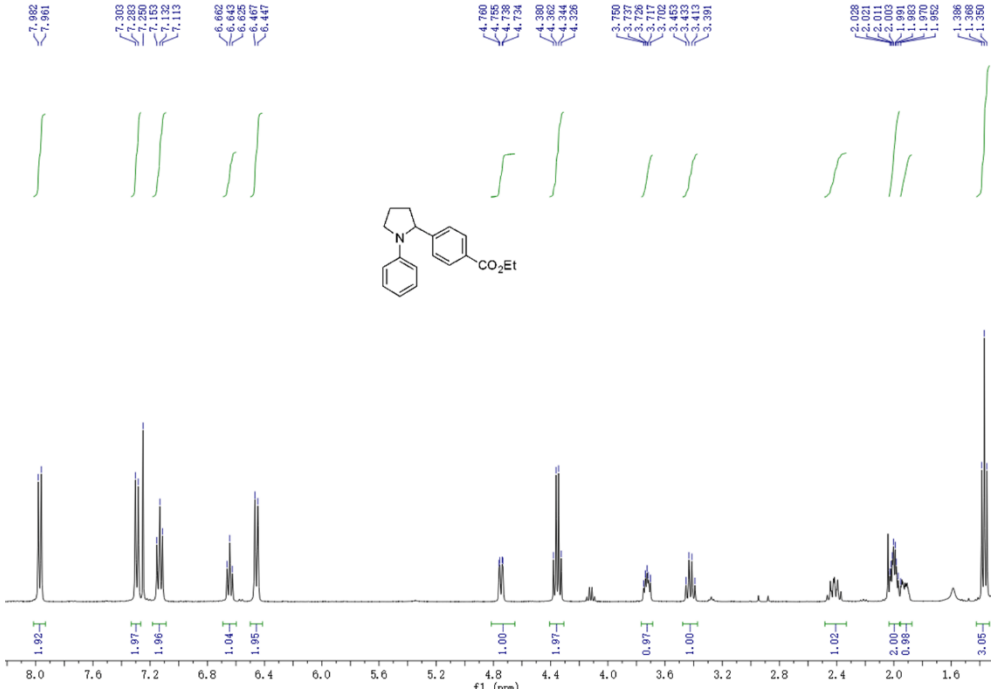

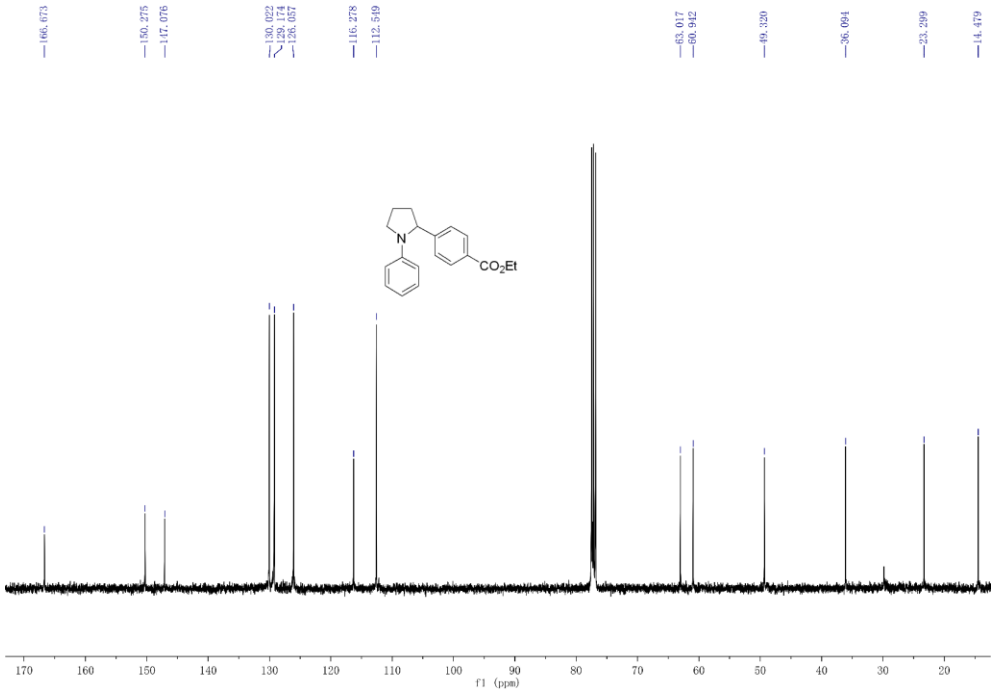

4-(1-Phenylpyrrolidin-2-yl)pyridine (3f)

^{1}H NMR (400 MHz, CDCl3) δ 8.51-8.49 (d, *J* = 6.0 Hz, 2H, Ar<u>H</u>), 7.17-7.13 (m, 4H, Ar<u>H</u>), 6.68-6.65 (t, *J* = 7.2 Hz, 1H, Ar<u>H</u>), 6.45-6.43 (d, *J* = 8.0, 2H, Ar<u>H</u>), 4.68-4.66 (dd, *J* = 9.2, 2.0 Hz, 1H, C<u>H</u>(Py)), 3.73-3.69 (m, 1H, C<u>H</u>$_A$H$_B$N), 3.44-3.38 (m, 1H, CH$_A$<u>H</u>$_B$N), 2.47-2.37 (m, 1H, C<u>H</u>$_A$CH$_B$CH(Ar)), 2.03-1.89 (m, 3H, CH$_A$C<u>H</u>$_B$CH(Ar) and C<u>H</u>$_2$CH$_2$N). **^{13}C NMR** (126 MHz, CDCl$_3$) *δ* 153.99 (C$_{Ar}$), 149.97 (C$_{Ar}$), 146.82 (C$_{Ar}$), 129.18 (C$_{Ar}$), 121.36 (C$_{Ar}$), 116.52 (C$_{Ar}$), 112.48 (C$_{Ar}$), 62.20 (<u>C</u>HPy), 49.23 (N<u>C</u>H$_2$), 35.59 (NCH$_2$CH$_2$<u>C</u>H$_2$), 23.22 (NCH$_2$<u>C</u>H$_2$).

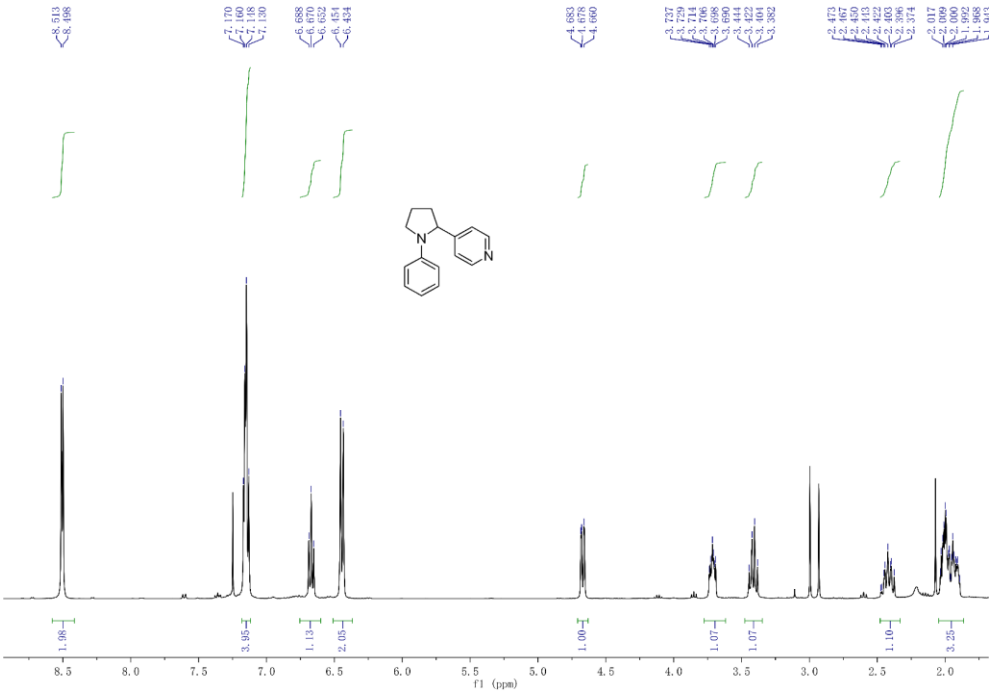

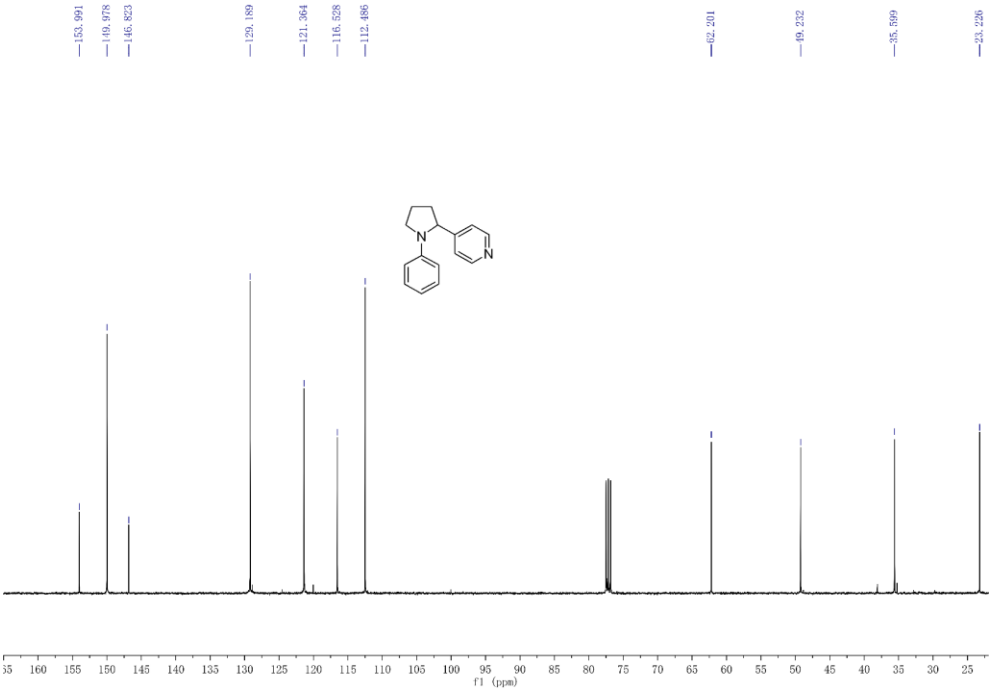

4-(phenyl-1-pyrrolidinylmethyl)benzonitrile (isomer 1 of 3g)

^{1}H NMR (400 MHz, CDCl3) δ 7.60-7.52 (q, J = 7.6 Hz, 4H, Ar<u>H</u>), 7.41-7.39 (d, J = 7.5 Hz, 2H, Ar<u>H</u>), 7.27-7.25 (d, J = 6.7 Hz, 2H, Ar<u>H</u>), 7.20-7.17 (t, J = 7.4 Hz, 1H, Ar<u>H</u>), 4.21 (s, 1H, CH(Ph-4-CN)), 2.41-2.38 (t, J = 5.5 Hz, 4H, $CH_2C\underline{H}_2NC\underline{H}_2CH_2$), 1.82-1.73 (m, 4H, $C\underline{H}_2CH_2NCH_2C\underline{H}_2$). **^{13}C NMR** (126 MHz, $CDCl_3$) δ 149.89 (C_{Ar}), 142.98 (C_{Ar}), 132.48 (C_{Ar}), 128.79 (C_{Ar}), 128.29 (C_{Ar}), 127.61 (C_{Ar}), 127.55 (C_{Ar}), 119.06 (C_{Ar}), 110.74 (CN), 76.12 (<u>C</u>H(Ph-4-CN)), 53.60 (2×$N\underline{C}H_2CH_2$), 23.67 (2×$NCH_2\underline{C}H_2$).

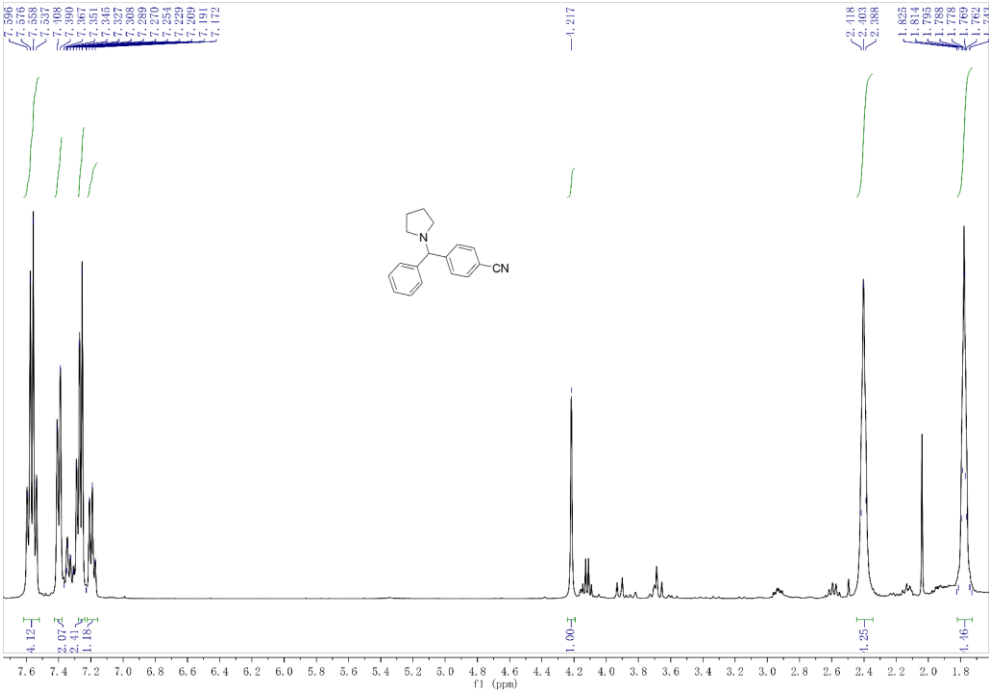

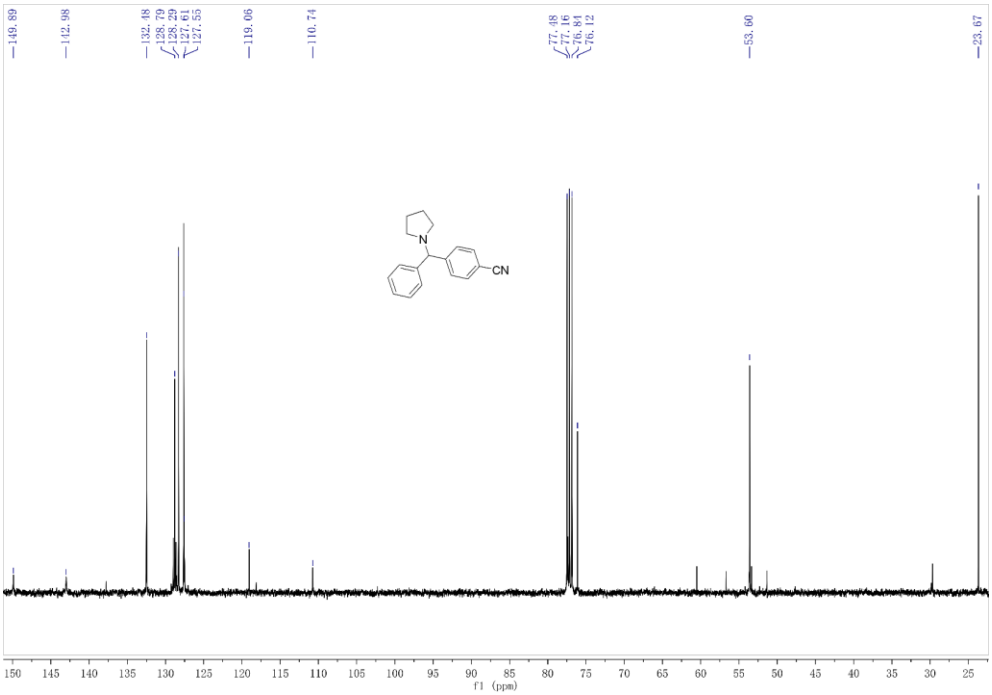

4-[1-(phenylmethyl)-2-pyrrolidinyl]benzonitrile (isomer 2 of 3g)

^{1}H NMR (400 MHz, $CDCl_3$) δ 7.63-7.61 (d, *J* = 7.6 Hz, 2H, Ar<u>H</u>),), 7.58-7.55 (d, *J* = 7.7 Hz, 2H, Ar<u>H</u>),), 7.38-7.18 (m, 5H, Ar<u>H</u>),), 3.77-3.74 (d, *J* = 13.07 Hz, 1H, CH(Ph-4-CN)), 3.49-3.45 (t, *J* = 8.26 Hz, 1H, C<u>H</u>$_A$H$_B$N), 3.15-3.10 (m, 2H, C<u>H</u>$_A$CH$_B$CH(Ph-4-CN) and CH$_A$<u>H</u>$_B$N, 2.30-2.15 (m, 2H, Ph-C<u>H</u>$_2$-N), 1.98-1.58 (m, 3H, CH$_A$C<u>H</u>$_B$CH(Ph-4-CN) and C<u>H</u>$_2$CH$_2$N). The isomer 2 of **3g** was not separable with 1-benzylpyrrolidine-2-carbonitrile, the decomposition product of starting material.

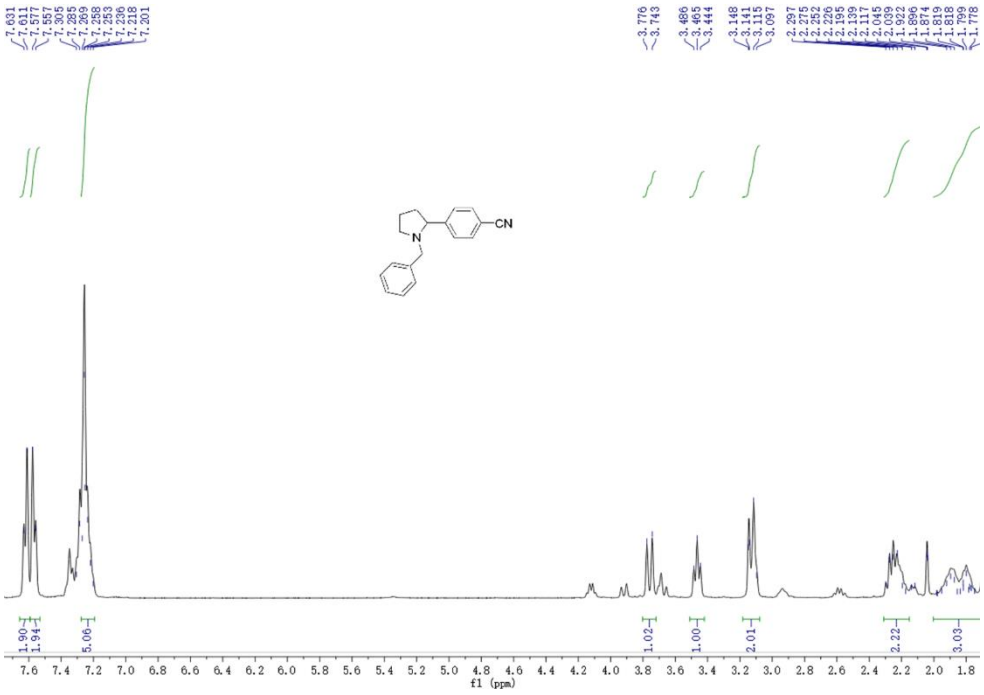

1-phenyl-2-Pyrrolidinone (4a)

^{1}H NMR (400 MHz, $CDCl_3$) *δ* 7.61 (d, *J* = 7.9 Hz, 2H, Ar<u>H</u>), *δ* 7.36 (t, *J* = 7.6 Hz, 2H, Ar<u>H</u>), *δ* 7.14 (t, *J* = 7.3 Hz, 1H, Ar<u>H</u>), *δ* 3.85 (t, *J* = 6.8 Hz, 2H, CH$_2$C<u>H</u>$_2$N), *δ* 2.60 (t, *J* = 7.9 Hz, 2H, C<u>H</u>$_2$CO), *δ* 2.15 (m, 2H, C<u>H</u>$_2$CH$_2$N). **^{13}C NMR** (126 MHz, $CDCl_3$) *δ* 174.20 (C=O), 139.45 (C_{Ar}), 128.82 (C_{Ar}), 124.49 (C_{Ar}), 119.97 (C_{Ar}), 48.78 (N<u>C</u>H$_2$), 32.77 (NCH$_2$CH$_2$<u>C</u>H$_2$), 18.04 (NCH$_2$<u>C</u>H$_2$).

11. References:

1. M.-D. Zhang, C.-M. Di, L. Qin, X.-Q. Yao, Y.-Z. Li, Z.-J. Guo and H.-G. Zheng, *Crystal Growth & Design*, 2012, **12**, 3957-3963.
2. J. Canny, R. Thouvenot, A. Teze, G. Herve, M. Leparuloloftus and M. T. Pope, *Inorg Chem*, 1991, **30**, 976-981.
3. J. Canny, R. Thouvenot, A. Teze, G. Herve, M. Leparuloloftus and M. T. Pope, *Inorg. Chem.*, 1991, **30**, 976-981.
4. Z. Ming, Y. Wang, T. Zhang, L. Li, C. Duan and Z. Liu, *ChemCatChem*, 2020, DOI: 10.1002/cctc.202001346.
5. D. Shi, Z. Ming, Q. Wu, T. Lai, K. Zheng, C. He and J. Zhao, *Inorg. Chem. Commun.*, 2019, **100**, 125-128.
6. D. Shi, C. He, W. Sun, Z. Ming, C. Meng and C. Duan, *Chem. Commun.*, 2016, **52**, 4714-4717.
7. C. Hua, A. Baldansuren, F. Tuna, D. Collison and D. M. D'Alessandro, *Inorg. Chem.*, 2016, **55**, 7270-7280.
8. A. McNally, C. K. Prier and D. W. C. MacMillan, *Science*, 2011, **334**, 1114-1117.
9. X. M. Zhang, S. R. Yeh, S. Hong, M. Freccero, A. Albini, D. E. Falvey and P. S. Mariano, *J. Am. Chem. Soc.*, 1994, **116**, 4211-4220.